BIODIVERSITAS
Volume 25, Number 11, November 2024
Pages: 4438-4449

ISSN: 1412-033X
E-ISSN: 2085-4722
DOI: 10.13057/biodiv/d251143

Diversity of bioactive compounds from *Parmotrema xanthinum* as antimicrobial potential through in-vitro and in-silico assessment

OKY KUSUMA ATNI, ERMAN MUNIR♥, NURSAHARA PASARIBU
Department of Biology, Faculty of Mathematics and Natural Sciences, Universitas Sumatera Utara. Jl. Bioteknologi No. 1, Medan 20155, North Sumatera, Indonesia. Tel.: +62-618-214290, ♥email: erman@usu.ac.id

Manuscript received: 30 September 2024. Revision accepted: 23 November 2024.

Abstract. *Atni OK, Munir E, Pasaribu N. 2024. Diversity of bioactive compounds from* Parmotrema xanthinum *as antimicrobial potential through in-vitro and in-silico assessment. Biodiversitas 25: 4438-4449.* Lichens, integral to ecosystem diversity, are known for producing bioactive secondary metabolites with significant pharmacological applications, particularly in antimicrobial therapies. This study evaluates the antimicrobial potential of *Parmotrema xanthinum* through in vitro and in silico approaches, emphasizing its role in biodiversity and drug discovery. Methanol extracts of *P. xanthinum* were tested against Gram-negative and Gram-positive bacteria, as well as pathogenic yeast, using the disc diffusion method. The extracts exhibited notable antimicrobial activity, particularly against *Escherichia coli* (18.6 ± 0.44 mm) and *Salmonella enterica* serovar Typhi (15.8 ± 0.25 mm). Gas chromatography-mass spectrometry (GC-MS) analysis identified 29 bioactive compounds, evaluated for drug-likeness using Lipinski's rule of five and biological activity predictions. Molecular docking studies with penicillin-binding protein 3 (PBP3) of *Pseudomonas aeruginosa* (PDB ID: 6I1E) revealed strong binding affinities. Notably, benzenepropanoic acid, α-(2,5-dioxopyrrolo)-, exhibited a binding energy of -5.9 kcal/mol, while 2,2,3,3-tetramethylcyclopropanoic acid, phenyl ester, showed -5.2 kcal/mol. These findings highlight *P. xanthinum* as a valuable source of bioactive compounds with potential for combating bacterial resistance. Further investigations into its bioactive mechanisms, pharmacodynamics, and safety profiles are recommended to advance its development as a viable candidate for antimicrobial drug discovery.

Keywords: Antimicrobial, bioactive compounds, lichens, molecular docking, penicillin-binding protein 3

INTRODUCTION

Lichens are a consequence of a symbiotic connection between fungi (mycobionts) and one or more phototrophic algae or cyanobacteria (photobionts). Lichens represent approximately 20% of known fungal biodiversity, with lichenologists having identified over 19,000 species, and the rate of discovery continues to increase (Lücking et al. 2017). Lichen-forming fungi produce a wide range of secondary metabolites via various biosynthetic pathways, including the polyketide (e.g., depsidones, usnic acid, depsides, and xanthones), shikimic acid (e.g., cyclopeptides and pulvinic acid derivatives), and mevalonic acid (e.g., diterpenes, triterpenes, and steroids) pathways (Ranković and Kosanić 2019; Goga et al. 2020). These secondary metabolites are commonly found as crystals on the surface of cortical and medullary hyphal cell walls. Lichens contain unique bioactive compounds that aid in systematics and phylogeny. These compounds are used at several taxonomic levels, including species, subspecies, and generic ranks (Ranković and Kosanić 2021).

Lichens produce a wide range of natural compounds, including depsides, depsidones, dibenzofurans, quinones, chromones, carotenoids, polysaccharides, monosaccharides, and aliphatic acids (Millot et al. 2016; Tatipamula et al. 2021; Macedo et al. 2021; Ureña-Vacas et al. 2021; Badiali et al. 2023). These compounds protect lichens from external threats and have significant pharmacological potential, including antimicrobial properties (antibacterial, antifungal, and antiviral activities), as well as antioxidant, anti-inflammatory, and antiproliferative effects (Nguyen et al. 2014; Dandapat and Paul 2019; Maulidiyah et al. 2021; Ozturk et al. 2021; Mendili et al. 2022; Kello et al. 2023).

Parmotrema is a prominent genus within the parmeloid lichens belonging to the family Parmeliaceae. This family, the largest lichenized fungi, encompasses approximately 2,700 species distributed across 80 genera. Members of Parmeliaceae are known for their diverse array of chemical compounds and wide range of biological activities. Species of *Parmotrema* produce various compounds, including atranorin, usnic acid, orsellinates, gyrophoric acid, salazinic acid, and lobaric acid. These compounds are well-known for their significant pharmacological activities, as well as their phytochemical and pharmacological properties (Gómez-Serranillos et al. 2014). Extracts and isolated compounds from various species within the *Parmotrema* genus have been demonstrated to possess certain antibacterial and antifungal activities (Tuan et al. 2020; Shiromi et al. 2021; Dwarakanath et al. 2022; Chakarwarti et al. 2024).

Several species of *Parmotrema* have demonstrated significant antimicrobial activities, with *Parmotrema tinctorum, Parmotrema cristiferum, Parmotrema grayanum,* and *Parmotrema praesorediosum* showing notable antifungal properties, and *Parmotrema grayanum, Parmotrema praesorediosum, Parmotrema tinctorum, Parmotrema reticulatum, Parmotrema pseudotinctorum, Parmotrema rampoddense,* and *Parmotrema dilatatum* exhibiting strong antibacterial activity (Saha et al. 2021).

Penicillin-binding proteins (PBPs), including 6I1E, identified as penicillin-binding protein 3 (PBP3) in *Pseudomonas aeruginosa*, are crucial for bacterial cell wall synthesis. They function as transpeptidases, carboxypeptidases, or endopeptidases during peptidoglycan formation and are essential for maintaining bacterial cell wall strength and integrity (Chen et al. 2017). PBP3 specifically catalyzes the transpeptidation of peptidoglycan synthesis. As a well-established target for β-lactam antibiotics, the inhibition of the activity of PBP3 disrupts cell wall synthesis and induces bacterial cell death. Amoxicillin, a β-lactam antibiotic, achieves this by covalently binding to the active site of PBP3, impairing its function and leading to bacterial lysis (Bellini et al. 2019).

The PDB structure 6I1E represents PBP3 from *P. aeruginosa* bound to an inhibitor and provides crucial insights into the binding interactions and mechanisms underlying the effects of these drugs. This structural information is essential for understanding how inhibitors affect PBP3 function and will aid the design of new antimicrobial agents and the development of strategies to combat bacterial resistance. Notably, lichen-derived metabolites with antimicrobial properties can inhibit PBP3 activity, much like synthetic antibiotics. This highlights the potential of lichen compounds to serve as natural alternatives in addressing the growing issue of bacterial resistance, offering new strategies to enhance treatment efficacy against resistant strains.

This study aimed to explore the bioactive compounds present in *Parmotrema xanthinum* and assess their potential as antimicrobial agents. By focusing on how these compounds interact with bacterial proteins through in silico methods, the research seeks to investigate and predict the effectiveness of these compounds as potential future drug candidates. The hypothesis is that the bioactive compounds in *P. xanthinum* could exhibit significant antimicrobial properties, providing a promising natural solution to combat bacterial resistance. By identifying key interactions and mechanisms, this research aims to contribute to the development of novel therapies derived from lichen species.

MATERIALS AND METHODS

Preparation of the lichen extracts

Parmotrema xanthinum samples were collected from the Bukit Barisan Grand Forest Park, North Sumatra, Indonesia (coordinates: 3.271120°N, 98.544043°E). The samples were cleaned and dried in an oven (UN 55 Universal Oven, Memmert, Germany) at 35°C for 4-5 days to eliminate water. The dried lichens were then ground using a blender. The lichen powder was then extracted by maceration with 70% methanol. This extraction process was conducted in three cycles, each lasting 24 hours, at room temperature, using a shaker set at 150 rpm. The filtrate containing the extract was separated from the residue using filter paper. Subsequently, the extract was concentrated using a rotary evaporator until a thick lichen extract was obtained. Finally, the concentrated lichen extract was diluted by 50% using dimethyl sulfoxide (DMSO) as the solvent.

Antimicrobial assays of lichens

Pathogens used for antimicrobial activity

Antimicrobial activity was evaluated using pathogenic microbes comprising three Gram-positive bacteria (*Staphylococcus aureus* ATCC 6538, *Propionibacterium acnes* ATCC 6919, and *Streptococcus mutans* ATCC 35668), three Gram-negative bacteria (*Salmonella enterica* serovar Typhi IPBCC b 11 669, *Escherichia coli* ATCC 8739, and *P. aeruginosa* ATCC 15442), and *Candida albicans* ATCC 10231.

Antibacterial activity

The antibacterial activity of lichen extract was evaluated using the disc diffusion method. Nutrient Agar (NA) medium (20 µL) was added into a Petri dish and allowed to solidify. A bacterial suspension was prepared with a turbidity equivalent to 0.5 McFarland standards. The suspension was evenly spread onto the surface of the agar medium using a sterile cotton swab. Discs containing 100 µL of the 50% lichen methanol extract were placed on the agar surface. Positive and negative controls were prepared with chloramphenicol and DMSO, respectively. Next, the Petri dishes were then incubated for 24 hours at room temperature. The inhibition zones around the discs were evaluated for the inhibition of bacterial growth.

Anti-Candida *activity*

The anti-Candida activity of lichen extract was tested using the disc diffusion method. Potato Dextrose Agar (PDA) medium (20 µL) was added into a Petri dish and allowed to solidify. *C. albicans* suspension was prepared with a turbidity equivalent 0.5 McFarland standards. The suspension was evenly spread onto the surface of the agar medium using a sterile cotton swab. Discs containing 100 µL of the 50% lichen methanol extract were placed on the agar surface. Positive and negative controls were prepared with ketoconazole and DMSO, respectively. Next, the Petri dishes were incubated for 48 hours at room temperature. The inhibition zones around the discs were measured to assess their activity against *C. albicans*.

GC-MS analysis

The sample filtered using a membrane filter was injected into a GC-MS instrument with a volume of 1 µL. Volatile component composition analysis was conducted using a Shimadzu GC-MS-QP2010 Plus, equipped with a split-splitless injector set at 250°C. The sample was injected using the split method, and the MS detector temperature was 280°C. The column used was a Restek Rtx-50 (Crossbond 5% phenyl-50% methyl polysiloxane) with an internal diameter of 0.25 mm, a length of 30 m, and a thickness of 0.25 µm. Helium was used as the carrier gas at a pressure of 64.1 kPa. The oven temperature program started at 80ºC with a 2-minute hold and ended at 280°C with an 8-minute hold. The total flow was 4.9 mL/min, with a column flow of 0.99 mL/min, linear velocity of 36.6 cm/sec, and purge flow of 3.0 mL/min. The mass spectrum of each detected compound peak in the chromatogram was

compared to that of known compounds in the Wiley9.LIB database.

Protein-ligand preparation

The bioactive compounds isolated from *P. xanthinum* used in this study were 9-octadecenal, (z)- (PubChem CID: 5364492), carbon dioxide (PubChem CID: 280), propanedioic acid (PubChem CID: 867), 2-heptene, 2,6-dimethyl- (PubChem CID: 521663), 2-butenoic acid (PubChem CID: 637090), 2-butenoic acid (PubChem CID: 637090), 6-oxabicyclo[3.1.0]hexan-2-one (PubChem CID: 242082), 2-octenal (PubChem CID: 5283324), cyclohexanol, 3,5-dimethyl- (PubChem CID: 21584), 6,8-dioxabicyclo(3.2.1)octan-2l-ol-2,3-d2 (242082), 7-tetradecene (PubChem CID: 5364651), the dimer of gamma-hydroxybutyric acid and crotyl ester, 6-methyl-6-nitro-2-heptanone (PubChem CID: 537587), isosorbide (PubChem CID: 12597), 2-(5'-hydroxy-1',1',5'-trimethylhexyl)-3-methylcyclopropenyl methyl ketone (PubChem CID: 5282854), (R)-(-)-(Z)-14-Methyl-8-hexadecen-1-ol (PubChem CID: 12487634). Additionally, benzenepropanoic acid, alpha-(2,5-dioxopyrrolo)- (PubChem CID: 319938), (1'-propenyl)thiophene (PubChem CID: 5371402), benzoic acid, 2-hydroxy-4-methoxy-3,5,6-trimethyl, methyl ester (PubChem CID: 606018), tetradecanoic acid (PubChem CID: 11005), hexadecanoic acid, methyl ester (PubChem CID: 8181), benzoic acid, 2,4-dihydroxy-6-methyl-, methyl ester (PubChem CID: 76658), tridecanoic acid (PubChem CID: 12530), 9,12-octadecadienoic acid (Z, Z)-, methyl ester (PubChem CID: 5284421), octadecanoic acid, ethyl ester (PubChem CID: 8122), 4N-methylamino-2(1H)-pyrimidinone (PubChem CID: 14803475), 9,12-octadecadienoic acid (Z, Z)- (PubChem CID: 5280450), 2,2,3,3-tetramethylcyclopropanoic acid, phenyl ester (PubChem CID: 97942), and 3-methyl-(2,6-dimethylheptyl)-2-penten-5-olide (PubChem CID: 10466745). Furthermore, compound 2-{1-[2-amino-2-(4-hydroxy-phenyl)-acetylamino]-2-oxo-ethyl}-5,5-dimethyl-thiazolidine-4-carboxylic acid (Control) (PubChem CID: 5287717) was used as a reference chemical to evaluate the inhibitory properties of the bioactive compounds obtained from *P. xanthinum*. The 2D and 3D structures of the active ingredients found in *P. xanthinum* and the control were acquired from the appropriate chemical databases on https://pubchem.ncbi.nlm.nih.gov. Subsequently, the structures were optimized for energy and transformed into the.pdb file format using Open Babel in PyRx software.

Biological activities prediction using Prediction of Activity Spectra for Substances (PASS) online

Prediction of the biological activity of the compound *P. xanthinum* was performed using the PASS server via the Way2 drug server (http://way2drug.com/PassOnline/). The prediction process involved obtaining the SMILES structure from PubChem (http://pubchem.ncbi.nlm.nih.gov) and submitting it to the Way2drug server. The following were the criteria for the PASS Online test's result (Pa-value): A Pa value >0.7 indicated a high probability of biological activity, while a Pa-value $0.5 \leq Pa \leq 0.7$ indicated low biological activity, and a Pa-value <0.5 indicated deficient activity.

Prediction of drug-likeness

The compounds' drug-likeness was assessed using Lipinski's rule of five. SwissADME (http://www.swissadme.ch/) was used to evaluate the drug-likeness of all compounds. This resource comprised parameters such as the number of hydrogen bond acceptors and donors, molecular weight, and bioavailability. Lipinski's rule of five facilitates the determination of whether a compound can be assimilated orally.

Molecular docking analysis

The study utilized AutoDock Vina within PyRx 8.0.0 for docking analysis, using the 6I1E protein as the macromolecule and evaluating bioactive compounds, along with 2-{1-[2-amino-2-(4-hydroxyphenyl)-acetylamino]-2-oxoethyl}-5,5-dimethyl-thiazolidine-4-carboxylic acid as a ligand (Bellini et al. 2019). Docking utilized specific grid parameters centered at (-0.7051×0.5977×0.3305) with dimensions (37.6127 Å×24.9049 Å×25.0000 Å). The docking outcomes were visualized using Discovery Studio 2024.

RESULTS AND DISCUSSION

Lichen morphology

Parmotrema xanthinum is a foliose lichen with bark as a substrate. The thallus was rounded with a smooth texture and uneven or wrinkled edges and did not fully adhere to the substrate. Cilia grew along the edges of the thallus, which measured between 10 and 27 cm in length and 1 and 5 cm in width and were gray-green. Reproductive structures were not observed (Figure 1). The chemical tests revealed that the upper cortex was yellow for K+, pink for C+, and red for KC+. This lichen is found in Indonesia, specifically in Taman Hutan Raya Bukit Barisan (Atni et al. 2024), Thailand, Cambodia, the Philippines, and Sri Lanka (Weerakoon and Aptroot 2014). It is a corticolous lichen typically found in areas with full sunlight at elevations of 875-908 m asl.

Figure 1. Morphology of *Parmotrema xanthinum* A. Thallus; B. Cilia

Antimicrobial activity of *P. xanthinum*

As shown in Table 1, the antimicrobial activity of the methanol extract of *P. xanthinum* against various pathogenic microorganisms demonstrated its diverse potential in combating infections. The largest inhibition zone was recorded against *E. coli* ATCC 8739 (18.6±0.44 mm) (Figure 2), indicating good effectiveness against Gram-negative bacteria and greater activity compared to that with *S. enterica* serovar Typhi IPBCC b 11 669 (15.8±0.25 mm) and *P. aeruginosa* ATCC 15442 (11.53±0.11 mm). This difference may be attributed to the ability of the extract to more effectively penetrate or disrupt the outer membrane and other specific targets in Gram-negative bacteria, which are generally more accessible to certain antimicrobial compounds than thicker peptidoglycan layers in Gram-positive bacteria. For Gram-positive bacteria, the extract showed significant activity with an inhibition zone of 16.13±0.24 mm against *S. mutans* ATCC 35668, compared to that against *P. acnes* ATCC 6919 (15.36±0.34 mm) and *S. aureus* ATCC 6538 (15.16±0.24 mm). Additionally, the extract exhibited antifungal activity against *C. albicans* ATCC 10231 with an inhibition zone of 8.96±0.32 mm, indicating its potential as an antifungal agent. These results suggested that the extract has diverse antimicrobial potential and may be more effective against Gram-negative than Gram-positive bacteria. However, further investigation is needed to understand its active compounds and mechanisms of action.

The larger inhibition zones for the growth of *E. coli* compared with that observed for the growth of other Gram-negative bacteria could be attributed to differences in the outer membrane composition and porin structures. *E. coli* may exhibit alterations in lipopolysaccharide (LPS) composition and porin loss, thereby affecting antimicrobial penetration (Choi and Lee 2019; Prajapati et al. 2021). Additionally, *E. coli* may have unique mechanisms, such as enzyme production and efflux systems, that influence its antibiotic susceptibility (Cunrath et al. 2019; Galindo-Méndez 2020). Changes in porin expression, such as reduced Outer Membrane Protein F (OmpF) levels, contribute to variations in inhibition zones (Alzayn et al. 2021). Strategies to overcome these barriers include the use of permeabilizers, such as Ethylenediaminetetraacetic acid (EDTA) and organic acids, to enhance antimicrobial efficacy by disrupting outer membrane permeability (Farrag et al. 2019; Zermeño-Cervantes et al. 2023). Furthermore, toxins produced by pathogenic bacteria are highly dangerous. *S. enterica* serovar Typhi produces cytolethal distending toxin (CDT), which damages DNA and requires bacterial internalization into host cells, while *E. coli* can produce Shiga toxin, causing diarrhea and cell damage (Smith et al. 2014; Thakur et al. 2022). Antimicrobial testing of *P. xanthinum* against pathogenic bacteria, especially those producing toxins, is crucial for preventing future infections.

GC-MS analysis

Raw GC-MS data and individual chromatograms were processed using Origin software. The GC-MS analysis revealed 29 bioactive compounds in *P. xanthinum*. These compounds were 9-octadecenal (z)-, carbon dioxide, propanedioic acid, 2-heptene (2,6-dimethyl-), 2-butenoic acid (repeated), 6-oxabicyclo[3.1.0]hexan-2-one, 2-octenal, cyclohexanol (3,5-dimethyl-), 6,8-dioxabicyclo(3.2.1)octan-2l-ol-2,3-d2, 7-tetradecene, a dimer of gamma-hydroxybutyric acid and crotyl ester, 6-methyl-6-nitro-2-heptanone, isosorbide, 2-(5'-hydroxy-1',1',5'-trimethylhexyl)-3-methylcyclopropenyl methyl ketone, (R)-(-)-(Z)-14-methyl-8-hexadecen-1-ol, benzenepropanoic acid (alpha-(2,5-dioxopyrrolo)-), (1'-propenyl)thiophene, benzoic acid (2-hydroxy-4-methoxy-3,5,6-trimethyl-, methyl ester), tetradecanoic acid, hexadecanoic acid (methyl ester), benzoic acid (2,4-dihydroxy-6-methyl-, methyl ester), tridecanoic acid, 9,12-octadecadienoic acid (Z,Z)- (methyl ester), octadecanoic acid (ethyl ester), 4N-methylamino-2(1H)-pyrimidinone, 9,12-octadecadienoic acid (Z,Z), 2,2,3,3-tetramethylcyclopropanoic acid (phenyl ester), and 3-methyl-(2,6-dimethylheptyl)-2-penten-5-olide.

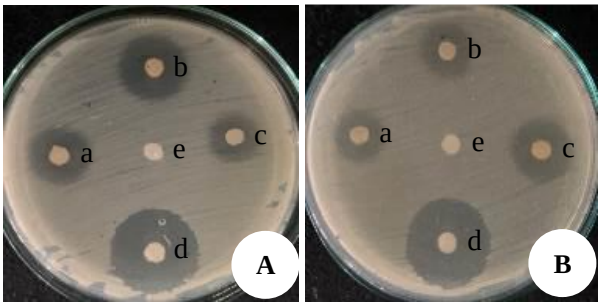

Figure 2. Inhibition zones of the methanol extract of *Parmotrema xanthinum* against A. Gram-negative bacteria *E. coli* ATCC 8739 (a-c: Replicates of the methanol extract of *P. xanthinum*, d: Positive control (chloramphenicol), e: Negative control (dimethyl sulfoxide); B. Gram-positive bacteria *S. mutans* ATCC 35668 (a-c: Replicates of methanol extract of *P. xanthinum*, d: positive control (chloramphenicol), e: negative control (dimethyl sulfoxide)

Table 1. Antimicrobial activity of methanol extract from *Parmotrema xanthinum*

Extract	Microorganism		Inhibition zone (mm)		
			Methanol extract (10 µL/disk)	Chlor-amphenicol	Keto-conazole
Parmotrema xanthinum	Gram-negative bacteria	*Salmonella enterica* serovar Typhi IPBCC b 11 669	15.8±0.25	31.76	
		Escherichia coli ATCC 8739	18.6±0.44	29.13	
		Pseudomonas aeruginosa ATCC 15442	11.53±0.11	26.53	
	Gram-positive bacteria	*Staphylococcus aureus* ATCC 6538	15.16±0.24	31.16	
		Propionibacterium acnes ATCC 6919	15.36±0.34	37.43	
		Streptococcus mutans ATCC 35668	16.13±0.24	22.8	
	Pathogenic yeast	*Candida albicans* ATCC 10231	8.96±0.32		40.83

The retention times are listed in Table 2, and the chromatograms are shown in Figure 3. According to a screening in PubChem, certain compounds lack existing 3D structures; therefore, 24 of the compounds listed in the database were utilized for docking analysis.

Prediction of compound biological activities

Numerous bioactive compounds from *P. xanthinum* showed significant potential for antimicrobial applications, as highlighted using PASS online analysis (Table 3). One of the most prominent compounds, benzenepropanoic acid, α-(2,5-dioxopyrrolo)-, stood out with a high probability of activity (Pa) of 0.901 for inhibiting muramoyltetrapeptide carboxypeptidase. This enzyme plays a critical role in bacterial cell wall synthesis, and its inhibition can disrupt bacterial growth, making it a strong candidate for antimicrobial therapy. Additionally, the compound showed the potential to inhibit Tpr proteinase with a Pa of 0.828, further supporting its role in targeting bacterial proteins involved in pathogenicity. These activities suggest that benzenepropanoic acid, α-(2,5-dioxopyrrolo)-, could effectively combat bacterial infections, particularly those resistant to conventional treatments.

However, certain compounds exhibited lower antimicrobial potentials. For instance, 9-octadecenal (Z)- showed moderate anti-infective activity, with a Pa of 0.781, but a lower antifungal activity, with a Pa of 0.566. Similarly, 2-heptene, 2,6-dimethyl-, demonstrated antifungal activity with a Pa of 0.516, which is considered low. Although these compounds possess certain antimicrobial properties, their efficacy in broad-spectrum antimicrobial treatments may be limited. Overall, the bioactive compounds from *P. xanthinum* exhibited a promising range of antimicrobial activities, although further refinement and optimization are necessary to enhance their therapeutic potential.

Table 2. Compounds isolated from *Parmotrema xanthinum*

Compound name	Mol. formula	Mass (g/mol)	R. time (min)	Area (%)	Smiles	PubChem ID
9-octadecenal, (z)-	$C_{18}H_{34}O$	266	0.174	0.03	CCCCCCCCC: CCCCCCCCC=O	5364492
Carbon dioxide	CO_2	118	1.799	0.11	C(=O)=O	280
Propanedioic acid	$C_3H_4O_4$	104	3.18	3.45	C(C(=O)O)C(=O)O	867
2-Heptene, 2,6-dimethyl-	C_9H_{18}	126	4.273	0.79	CC(C)CCC=C(C)C	521663
2-Butenoic acid	$C_4H_6O_2$	86	7.29	0.37	CC=CC(=O)O	637090
2-Butenoic acid	$C_4H_6O_2$	86	8.403	4.34	CC=CC(=O)O	637090
6-Oxabicyclo[3.1.0]hexan-2-one	$C_5H_6O_2$	98	9.997	0.58	C1CC(=O)C2C1O2	242082
2 octenal	$C_8H_{14}O$	126	10.896	0.28	CCCCCC=CC=O	5283324
Cyclohexanol, 3,5-dimethyl-	$C_8H_{16}O$	128	13.099	0.16	CC1CC(CC(C1)O)C	21584
6,8-dioxabicyclo(3.2.1)octan-2l-ol-2,3-d2	$C_6H_8D_2O_3$	130	14.588	0.65	-	-
7-tetradecene	$C_{14}H_{28}$	196	16.629	0.29	CCCCCCC=CCCCCCC	5364651
Dimer of gamma-hydroxy butyric acid, crotyl ester, and gamma-hydroxy-methyl	$C_9H_{14}O_4$	186	17.423	0.20	-	-
6-methyl-6-nitro-2-heptanone	$C_8H_{15}NO_3$	173	18.481	0.24	CC(=O)CCCC(C)(C)[N+](=O)[O-]	537587
Isosorbide	$C_6H_{10}O_4$	146	20.305	1.24	C1C(C2C(O1)C(CO2)O)O	12597
2-(5'-Hydroxy-1',1',5'-trimethylhexyl)-3-methyl cyclopropenyl methyl ketone	$C_{14}H_{24}O_2$	224	23.603	1.73	C1CC(C=C1)CCCCCCCCC(=O)O	5282854
(R)-(-)-(Z)-14-Methyl-8-hexadecen-1-ol	$C_{17}H_{34}O$	254	24.839	0.24	CCC(C)CCCCC=CCCCCCCCO	12487634
Benzenepropanoic acid,.alpha.-(2,5-dioxopyrrolo)-	$C_{13}H_{11}NO_4$	245	26.406	0.51	C1=CC=C(C=C1)CC(C(=O)O)N2C(=O)C=CC2=O	319938
(1'-propenyl)thiophene	C_7H_8S	124	27.927	15.89	CC=CC1=CC=CS1	5371402
Benzoic acid, 2-hydroxy-4-methoxy-3,5,6-trimethyl-, methyl ester	$C_{12}H_{16}O_4$	224	30.133	2.30	CC1=C(C(=C(C(=C1C(=O)OC)O)C)OC)C	606018
Tetradecanoic acid	$C_{14}H_{28}O_2$	228	30.618	3.35	CCCCCCCCCCCCCC(=O)O	11005
Hexadecanoic acid, methyl ester	$C_{17}H_{34}O_2$	270	31.408	9.70	CCCCCCCCCCCCCCCC(=O)OC	8181
Benzoic acid, 2,4-dihydroxy-6-methyl-, methyl ester	$C_9H_{10}O_4$	182	32.963	12.16	CC1=CC(=CC(=C1C(=O)OC)O)O	76658
Tridecanoic acid	$C_{13}H_{26}O_2$	214	34.564	7.58	CCCCCCCCCCCCC(=O)O	12530
9,12-Octadecadienoic acid (Z,Z)-, methyl ester	$C_{19}H_{34}O_2$	294	35.341	9.88	CCCCCC=CCC=CCCCCCCCC(=O)OC	5284421
Octadecanoic acid, ethyl ester	$C_{20}H_{40}O_2$	312	36.368	4.60	CCCCCCCCCCCCCCCCCC(=O)OCC	8122
4N-methylamino-2(1H)-pyrimidinone	$C_5H_7N_3O$	125	37.437	5.55	CNC1=NC=CC(=O)N1	14803475
9,12-Octadecadienoic acid (Z,Z)-	$C_{18}H_{32}O_2$	280	38.205	4.18	CCCCCC=CCC=CCCCCCCCC(=O)O	5280450
2,2,3,3-Tetramethylcyclo-propanoic acid, phenyl ester	$C_{14}H_{18}O_2$	218	38.702	3.30	C1CCC(CC1)C(C2=CC=CC=C2)C(=O)O	97942
3-methyl-(2,6-dimethylheptyl)-2-penten-5-olide	$C_{15}H_{26}O_2$	238	39.542	6.31	CC(C)C1CCC(C2C1C(CC2)C(=O)C)(C)O	10466745

Table 3. Prediction of the biological activity of compounds from *Parmotrema xanthinum* via the pass online test

Compound name	Biological activity	Pa	Pi	Criteria
9-Octadecenal, (Z)-	Anti-infective	0.781	0.005	High
	Antifungal	0.566	0.022	Low
Carbon dioxide	-	-	-	-
Propanedioic acid	Poly(3-hydroxybutyrate) depolymerase inhibitor	0.850	0.002	High
	Acetylesterase inhibitor	0.851	0.004	High
2-Heptene, 2,6-dimethyl-	Acylcarnitine hydrolase inhibitor	0.723	0.023	High
	Antifungal	0.516	0.028	Low
2-Butenoic acid	Phosphatidylglycerophosphatase inhibitor	0.810	0.003	High
	Licheninase inhibitor	0.719	0.004	High
6-Oxabicyclo[3.1.0]hexan-2-one	Glucan 1,4-alpha-maltotriohydrolase inhibitor	0.810	0.004	High
	Histidine kinase inhibitor	0.755	0.005	High
2 octenal	Limulus clotting factor B inhibitor	0.771	0.006	High
	Acrocylindropepsin inhibitor	0.866	0.009	High
Cyclohexanol, 3,5-dimethyl-	Ubiquinol-cytochrome-c reductase inhibitor	0.898	0.005	High
	Antifungal	0.563	0.022	Low
7-Tetradecene	Antieczematic	0.954	0.002	High
	Chymosin inhibitor	0.926	0.004	High
6-methyl-6-nitro-2-heptanone	Gluconate 2-dehydrogenase (acceptor) inhibitor	0.933	0.003	High
	Saccharopepsin inhibitor	0.861	0.010	High
Isosorbide	Pectate Lyase Inhibitor	0.700	0.005	High
	Polyporopepsin inhibitor	0.756	0.028	High
2-(5'-Hydroxy-1',1',5'-trimethylhexyl)-3-methylcyclopropenyl methyl ketone	Dextranase inhibitor	0.814	0.005	High
	Antifungal	0.546	0.024	Low
(R)-(-)-(Z)-14-Methyl-8-hexadecen-1-ol	Exoribonuclease II inhibitor	0.767	0.010	High
	Antifungal	0.592	0.019	Low
Benzenepropanoic acid,.alpha.-(2,5-dioxopyrrolo)-	Muramoyltetrapeptide carboxypeptidase inhibitor	0.901	0.004	High
	Tpr proteinase (*Porphyromonas gingivalis*) inhibitor	0.828	0.003	High
(1'-propenyl)thiophene	Complement factor D inhibitor	0.933	0.002	High
	Feruloyl esterase inhibitor	0.681	0.023	Low
Benzoic acid, 2-hydroxy-4-methoxy-3,5,6-trimethyl-, methyl ester	Chlordecone reductase inhibitor	0.813	0.018	High
	Membrane integrity agonist	0.878	0.017	High
Tetradecanoic acid	Acrocylindropepsin inhibitor	0.961	0.002	High
	Glucan endo-1,3-beta-D-glucosidase inhibitor	0.945	0.002	High
Hexadecanoic acid, methyl ester	Saccharopepsin inhibitor	0.962	0.002	High
	Chymosin inhibitor	0.962	0.002	High
Benzoic acid, 2,4-dihydroxy-6-methyl-, methyl ester	Membrane integrity agonist	0.927	0.005	High
	Membrane permeability inhibitor	0.927	0.005	High
Tridecanoic acid	Lysostaphin inhibitor	0.855	0.003	High
	Chymosin inhibitor	0.961	0.002	High
9,12-Octadecadienoic acid (Z,Z)-, methyl ester	Pediculicide	0.717	0.003	High
	Antifungal	0.507	0.029	Low
4N-methylamino-2(1H)-pyrimidinone	Membrane permeability inhibitor	0.792	0.011	High
	Pterin deaminase inhibitor	0.804	0.004	High
9,12-Octadecadienoic acid (Z,Z)-	Peptidoglycan glycosyltransferase inhibitor	0.720	0.003	High
	Antifungal	0.500	0.030	Low
2,2,3,3-Tetramethylcyclopropanoic acid, phenyl ester	CYP2J substrate	0.863	0.009	High
	Acylcarnitine hydrolase inhibitor	0.831	0.010	High
3-methyl-(2,6-dimethylheptyl)-2-penten-5-olide	Membrane permeability inhibitor	0.671	0.052	Low
	Prostaglandin-E2 9-reductase inhibitor	0.765	0.012	High

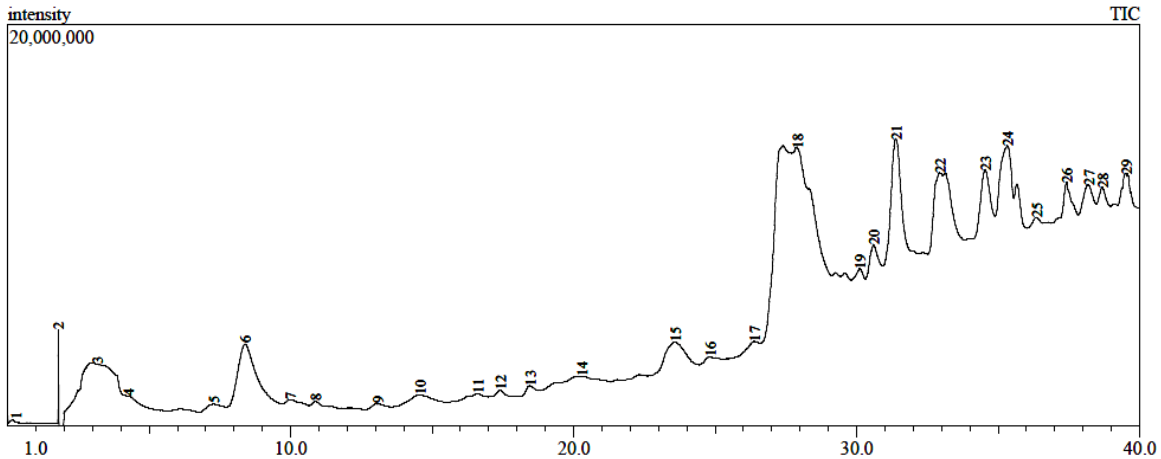

Figure 3. The GC-MS chromatogram of *Parmotrema xanthinum*

Prediction of drug-likeness

The analysis revealed varying adherence to the drug-likeness criteria among the compounds from *P. xanthinum* (Table 4). Compounds such as 9-octadecenal (z)- (MlogP 4.68), 2-heptene, 2,6-dimethyl- (MlogP 4.38), 9,12-octadecadienoic acid (Z,Z)- (MlogP 4.7), 7-tetradecene (MlogP 5.79), hexadecanoic acid, methyl ester (MlogP 4.44), and (R)-(-)-(Z)-14-methyl-8-hexadecen-1-ol (MlogP 4.55) deviated from Lipinski's rules primarily due to their elevated MlogP values, which exceeded the recommended threshold of 4.15. These high MlogP values indicated potential issues with permeability that may affect the drug-like properties. Conversely, compounds such as 2-octenal (MlogP=1.97), cyclohexanol, 3,5-dimethyl- (MlogP=1.83), and 6-oxabicyclo[3.1.0]hexan-2-one (MlogP=-0.31) adhered to Lipinski's rules, with MlogP values well below the threshold and hydrogen bond counts within acceptable limits, suggesting good potential for oral bioavailability.

High MlogP values often lead to excessive lipophilicity, presenting significant challenges to drug absorption, distribution, metabolism, and excretion. The 'rule of five' proposed by Lipinski et al. (1997) plays a crucial role in this context, predicting that poor absorption and permeation are more likely when logP exceeds certain thresholds, and high lipophilicity can result in suboptimal pharmacokinetic properties. Recent studies have further emphasized these findings, indicating that compounds with high MlogP values often encounter challenges in drug development and necessitate optimization to enhance their pharmacokinetic characteristics and overall drug-likeness. These insights underline the importance of refining the molecular properties of drug candidates to improve their efficacy and safety profiles (Ivanović et al. 2020; Karami et al. 2022).

Lipinski's rule was used to evaluate the physicochemical features of *P. xanthinum* compounds, and 19 of the 25 compounds met the criteria for drug-like qualities (Table 4). This is promising for medicinal applications, such as antibacterial usage. Adherence to Lipinski's criteria is critical because these criteria typically correspond to ideal absorption, distribution, metabolism, and excretion (ADME) profiles, which are required for designing effective and safe drugs.

Molecular interactions of bioactive compounds *Parmotrema xanthinum* with 6I1E

The control substances were compared based on the molecular docking modeling results. 2-{1-[2-Amino-2-(4-hydroxy-phenyl)-acetylamino]-2-oxo-ethyl}-5,5-dimethyl-thiazolidine-4-carboxylic acid and several bioactive compounds from *P. xanthinum* showed substantial differences in the type of interaction and binding energy to protein targets. As a control compound, 2-{1-[2-amino-2-(4-hydroxy-phenyl)-acetylamino]-2-oxo-ethyl}-5,5-dimethyl-thiazolidine-4-carboxylic acid had the highest binding energy of all the chemicals examined, at -6.3 kcal/mol. The major contacts were hydrogen bonds with residues SER435, THR437, and ARG438, hydrophobic interactions with residues LEU 219 and VAL439, and electrostatic interactions with residue TRP185. This demonstrated its great affinity for the target. 2-{1-[2-Amino-2-(4-hydroxy-phenyl)-acetylamino] -2-oxo-ethyl-5,5-dimethyl-thiazolidine-4-carboxylic acid efficiently inhibited the activity of the target protein (Table 5) (Figures 4 and 5).

Table 4. Physicochemical properties of compounds from *Parmotrema xanthinum* based on Lipinski's rule of five

Compound name	Lipinski				
	MW	MlogP ≤ 4.15	NorO ≤ 10	NHorOH ≤ 5	Violasi
9-octadecenal, (z)-	266	4.68	1	0	Yes (1)
Carbon dioxide	118	-1.24	2	0	Yes (0)
Propanedioic acid	104	-0.99	4	2	Yes (0)
2-Heptene, 2,6-dimethyl-	126	4.38	0	0	Yes (1)
2-Butenoic acid	86	0.38	2	1	Yes (0)
6-Oxabicyclo[3.1.0]hexan-2-one	98	-0.31	2	0	Yes (0)
2 octenal	126	1.97	1	0	Yes (0)
Cyclohexanol, 3,5-dimethyl-	128	1.83	1	1	Yes (0)
7-tetradecene	196	5.79	0	0	Yes (0)
6-methyl-6-nitro-2-heptanone	173	0.59	3	0	Yes (0)
Isosorbide	146	-1.52	4	2	Yes (0)
2-(5'-Hydroxy-1',1',5'-trimethylhexyl)-3-methylcyclopropenyl methyl ketone	224	3.19	2	1	Yes (0)
(R)-(-)-(Z)-14-Methyl-8-hexadecen-1-ol	254	4.55	1	1	Yes (1)
Benzenepropanoic acid,.alpha.-(2,5-dioxopyrrolo)-(1'-propenyl)thiophene	245	0.74	4	1	Yes (0)
Benzoic acid, 2-hydroxy-4-methoxy-3,5,6-trimethyl-, methyl ester	124	2.17	0	0	Yes (0)
Tetradecanoic acid	224	1.93	4	1	Yes (0)
Hexadecanoic acid, methyl ester	228	3.69	2	1	Yes (0)
Benzoic acid, 2,4-dihydroxy-6-methyl-, methyl ester	270	4.44	2	0	Yes (1)
Tridecanoic acid	182	1.06	4	2	Yes (0)
9,12-Octadecadienoic acid (Z,Z)-, methyl ester	214	3.42	2	1	Yes (0)
4N-methylamino-2(1H)-pyrimidinone	294	4.7	2	0	Yes (1)
9,12-Octadecadienoic acid (Z,Z)-	125	-0.44	2	2	Yes (0)
2,2,3,3-Tetramethylcyclopropanoic acid, phenyl ester	280	4.47	2	1	Yes (1)
3-methyl-(2,6-dimethylheptyl)-2-penten-5-olide	218	3	2	1	Yes (0)
	238	2.74	2	1	Yes (0)

Notes: MW: Molecular weight (measured in g/mol); MlogP: Logarithm of the partition coefficient between octanol and water, indicating the lipophilicity of the compound; NorO: Number of oxygen atoms in the molecule; NHorOH: Number of nitrogen atoms and hydroxyl groups (OH) in the compound

In total, 24 bioactive compounds from *P. xanthinum* demonstrated diverse binding potentials for the 6I1E protein in molecular docking studies, highlighting their promising antimicrobial applications. Among these, benzenepropanoic acid, α-(2,5-dioxopyrrolo)-, exhibited the highest binding energy, surpassing the control compound, 2-{1-[2-amino-2-(4-hydroxyphenyl)-acetylamino]-2-oxoethyl}-5,5-dimethyl-thiazolidine-4-carboxylic acid (binding energy of -5.9 kcal/mol). benzenepropanoic acid, α-(2,5-dioxopyrrolo)- higher binding energy can be attributed to its stable interactions with key protein residues, including hydrogen bonds with ALA220, THR437, and ARG438, and hydrophobic interactions with TRP185, which enhance the stability of the ligand-protein complex.

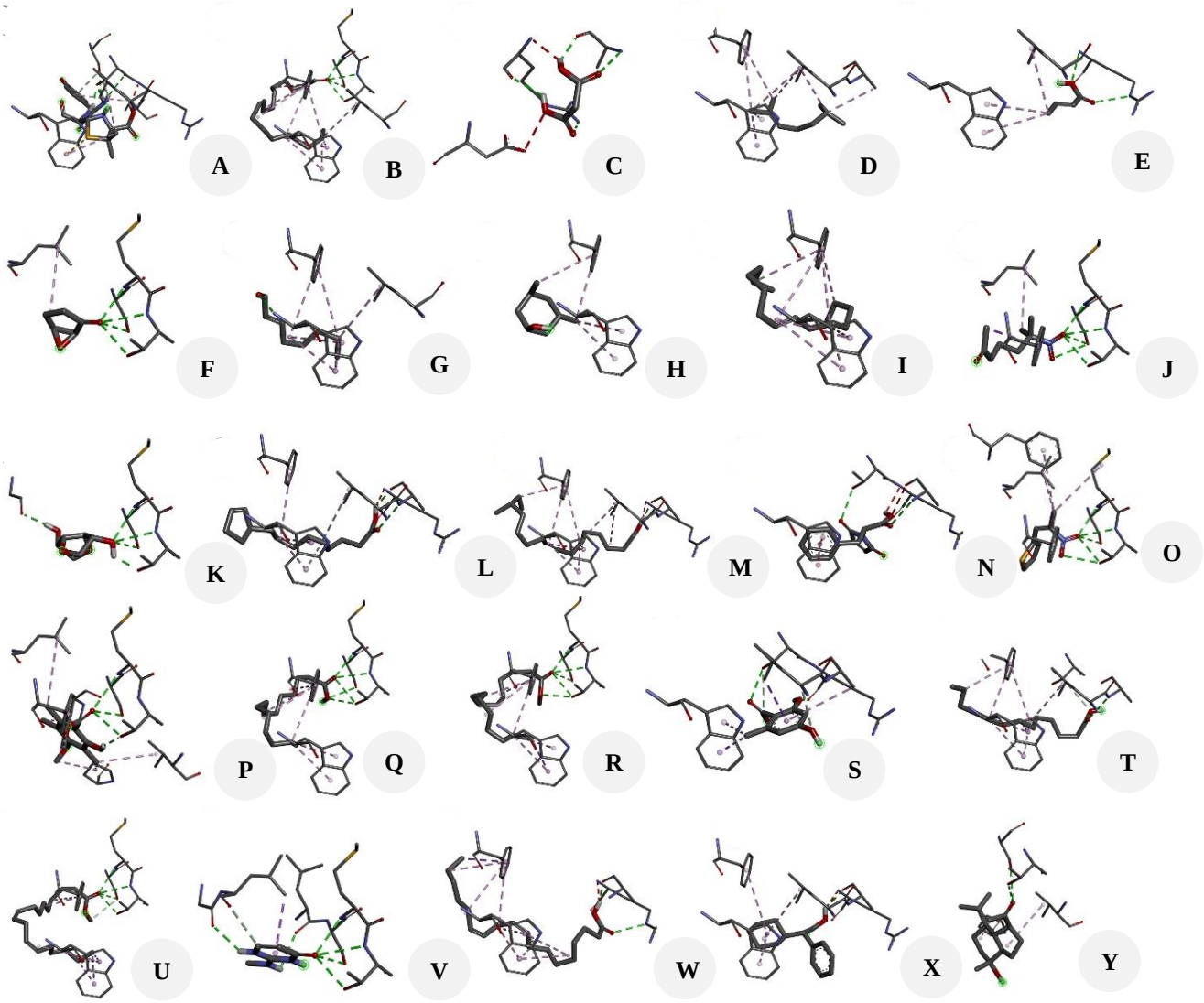

Figure 4. The 3D interactions of 2-{1-[2-amino-2-(4-hydroxy-phenyl)-acetylamino]-2-oxo-ethyl}-5,5-dimethyl-thiazolidine-4-carboxylic acid (control) and bioactive compounds from *Parmotrema xanthinum* against the 6I1E protein. A. 2-{1-[2-amino-2-(4-hydroxy-phenyl)-acetylamino]-2-oxo-ethyl}-5,5-dimethyl-thiazolidine-4-carboxylic acid; B. 9-octadecenal, (z)-; C. Propanedioic acid; D. 2-heptene, 2,6-dimethyl-; E. 2-butenoic acid; F. 6-oxabicyclo[3.1.0]hexan-2-one; G. 2 octenal; H. Cyclohexanol, 3,5-dimethyl-; I. 7-tetradecene; J. 6-methyl-6-nitro-2-heptanone; K. Isosorbide; L. 2-(5'-hydroxy-1',1',5'-trimethylhexyl)-3-methylcyclopropenyl methyl ketone; M. (R)-(-)-(Z)-14-methyl-8-hexadecen-1-ol; N. Benzenepropanoic acid,. alpha.-(2,5-dioxopyrrolo)-; O. (1'-propenyl)thiophene; P. Benzoic acid, 2-hydroxy-4-methoxy-3,5,6-trimethyl-, methyl ester; Q. Tetradecanoic acid; R. Hexadecanoic acid, methyl ester; S. Benzoic acid, 2,4-dihydroxy-6-methyl-, methyl ester; T. Tridecanoic acid; U. 9,12-octadecadienoic acid (Z,Z)-, methyl ester; V. 4N-methylamino-2(1H)-pyrimidinone; W. 9,12-octadecadienoic acid (Z,Z)-; X. 2,2,3,3-tetramethylcyclopropanoic acid, phenyl ester; Y. 3-methyl-(2,6-dimethylheptyl)-2-penten-5-olide

Table 5. Residue and binding energies of the ligand and 6I1E interaction

Ligands	Interaction type					Binding affinity
	Hydrogen bond		Hydrophobic	Electrostatic	Unfavorable	
	Hydrogen bond	Carbon hydrogen bond				
Control						
2-{1-[2-Amino-2-(4-hydroxy-phenyl)-acetylamino]-2-oxo-ethyl}-5,5-dimethyl-thiazolidine-4-carboxylic acid	SER435, THR437, ARG438	-	LEU219, VAL439	TRP185	-	-6.3
Bioactive components of the *P. xanthinum*						
9-Octadecenal, (Z)-	SER435, MET436, THR437	-	PHE182, TRP185, LEU219	-	-	-4.4
Propanedioic acid	ALA220, ARG438	-	-	-	ASP440	-3.6
2-Heptene, 2,6-dimethyl-	-	-	PHE182, TRP185, LEU 219, ALA220	-	-	-3.6
2-Butenoic acid	THR218, ALA220, ASP440, THR437, ARG438	-	TRU489	-	-	-3.2
6-Oxabicyclo[3.1.0]hexan-2-one	SER435, THR437, MET436	-	LEU381	-	-	-3.7
2 octenal	TRP182	-	PHE182, LEU219	-	-	-3.6
Cyclohexanol, 3,5-dimethyl-	-	-	PHE182, TRP185	-	-	-3.7
7-Tetradecene	-	-	PHE182, TRP185	-	-	-3.8
6-methyl-6-nitro-2-heptanone	SER435, MET436, THR437	-	PHE182, LEU381	-	-	-4.6
Isosorbide	SER435, MET436, THR437, GLY380	-	-	-	-	-4
2-(5'-Hydroxy-1',1',5'-trimethylhexyl)-3-methylcyclopropenyl methyl ketone	ALA220	-	PHE182, TRP185, LEU219	-	ARG 438	-5
(R)-(-)-(Z)-14-Methyl-8-hexadecen-1-ol	ALA220	-	PHE182, TRP185, LEU219	-	ARG 438	-4.4
Benzenepropanoic acid,.alpha.-(2,5-dioxopyrrolo)-	ALA220, THR437, ARG438	-	TRP 185	-	-	-5.9
(1'-propenyl)thiophene	SER435, MET436, THR437	-	PHE182, LEU381, PHE383	-	-	-4.2
Benzoic acid, 2-hydroxy-4-methoxy-3,5,6-trimethyl-, methyl ester	SER435, MET436, THR437	-	PHE182, LEU381, PRO433, PRO443, VAL439	-	-	-4.6
Tetradecanoic acid	SER435, MET436, THR437	-	PHE182, TRP185	-	-	-4.2
Hexadecanoic acid, methyl ester	SER435, MET436, THR437	-	PHE182, TRP185	-	-	-4.3
Benzoic acid, 2,4-dihydroxy-6-methyl-, methyl ester	LEU219, THR437, ARG438	-	TRP185, ALA220	-	-	-4.9
Tridecanoic acid	ALA220, THR437	-	PHE182, TRP185, LEU219	-	-	-4.5
9,12-Octadecadienoic acid (Z,Z)-, methyl ester	SER435, MET436, THR437	-	PHE182, TRP185	-	-	-4.6
4N-methylamino-2(1H)-pyrimidinone	GLY380, LEU434, SER435, MET436, THR437	LEU381	-	-	-	-4.4
9,12-Octadecadienoic acid (Z,Z)-	ALA220, ARG438	-	PHE182, TRP185	-	-	-5.1
2,2,3,3-Tetramethylcyclopropanoic acid, phenyl ester	ALA220	-	PHE182, TRP185, LEU219	-	ARG438	-5.2
3-methyl-(2,6-dimethylheptyl)-2-penten-5-olide	SER435, THR437	-	VAL439, PRO443	-	-	-4.8

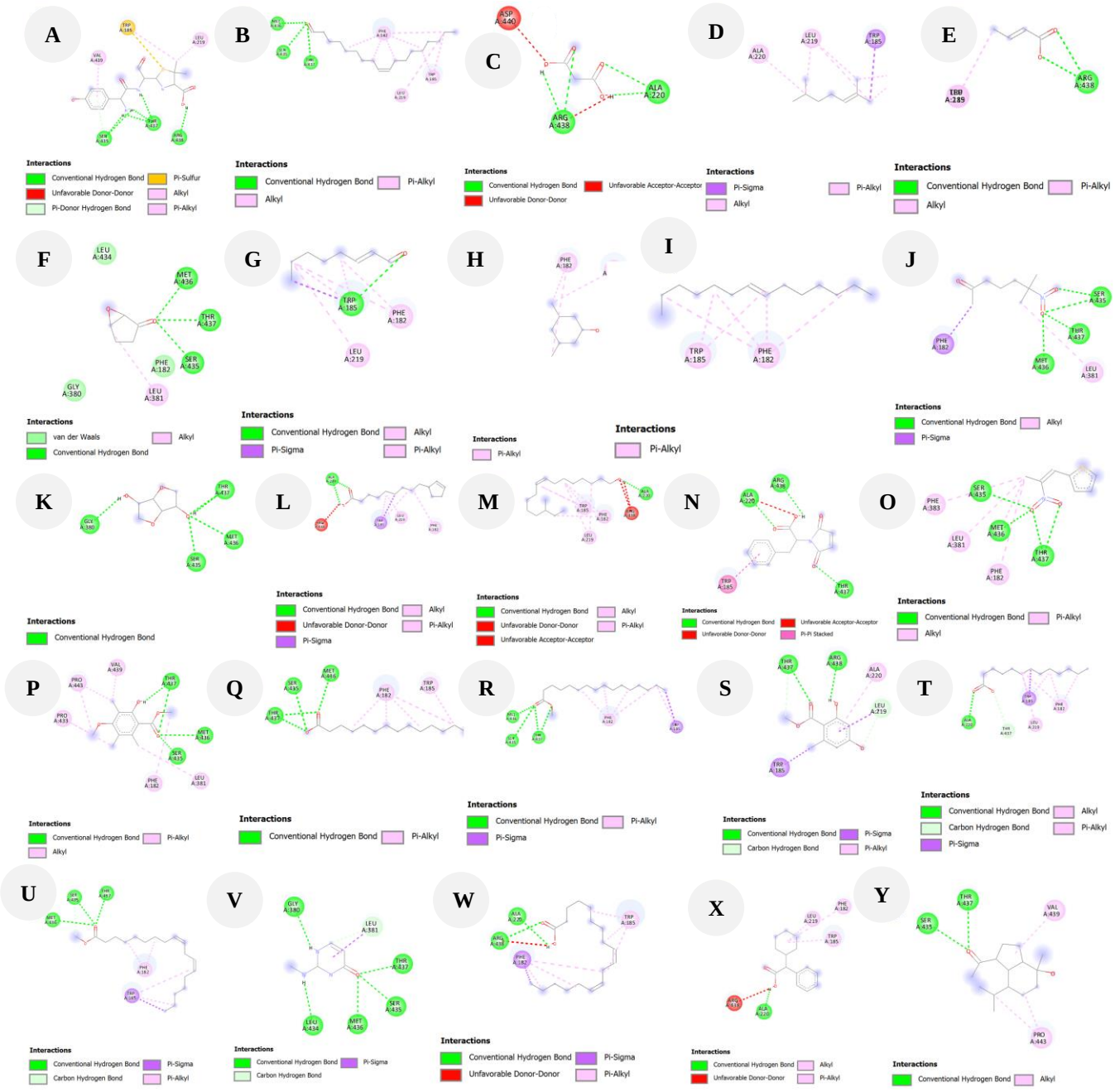

Figure 5. 2D interactions of 2-{1-[2-amino-2-(4-hydroxy-phenyl)-acetylamino]-2-oxo-ethyl}-5,5-dimethyl-thiazolidine-4-carboxylic acid (control) and bioactive compounds from *Parmotrema xanthinum* against the 6I1E protein. A. 2-{1-[2-amino-2-(4-hydroxy-phenyl)-acetylamino]-2-oxo-ethyl}-5,5-dimethyl-thiazolidine-4-carboxylic acid; B. 9-octadecenal, (z)-; C. Propanedioic acid; D. 2-heptene, 2,6-dimethyl-; E. 2-butenoic acid; F. 6-oxabicyclo[3.1.0]hexan-2-one; G. 2 octenal; H. Cyclohexanol, 3,5-dimethyl-; I. 7-tetradecene; J. 6-methyl-6-nitro-2-heptanone; K. Isosorbide; L. 2-(5'-hydroxy-1',1',5'-trimethylhexyl)-3-methylcyclopropenyl methyl ketone; M. (R)-(-)-(Z)-14-Methyl-8-hexadecen-1-ol; N. Benzenepropanoic acid,. alpha.-(2,5-dioxopyrrolo)-; O. (1'-propenyl)thiophene; P. Benzoic acid, 2-hydroxy-4-methoxy-3,5,6-trimethyl-, methyl ester; Q. Tetradecanoic acid; R. Hexadecanoic acid, methyl ester; S. Benzoic acid, 2,4-dihydroxy-6-methyl-, methyl ester; T. Tridecanoic acid; U. 9,12-octadecadienoic acid (Z,Z)-, methyl ester; V. 4N-methylamino-2(1H)-pyrimidinone; W. 9,12-octadecadienoic acid (Z,Z)-; X. 2,2,3,3-tetramethylcyclopropanoic acid, phenyl ester; Y. 3-methyl-(2,6-dimethylheptyl)-2-penten-5-olide

These strong interactions, especially with both polar and hydrophobic residues, contribute to its higher binding affinity, positioning benzenepropanoic acid as a promising antimicrobial candidate. In contrast, 2,2,3,3-tetramethylcyclopropanoic acid, phenyl ester, with a slightly lower binding energy (-5.2 kcal/mol), also demonstrated significant binding potential and could serve as a candidate for antimicrobial activity. This compound formed hydrogen bonds with ALA220 and hydrophobic interactions with PHE182, TRP185, and LEU219, but unfavorable interactions

with ARG438 may have slightly destabilized the complex, reducing its binding affinity compared to benzenepropanoic acid. Nonetheless, its interactions suggest that further optimization could enhance its antimicrobial potential.

In contrast, some compounds exhibited lower binding affinities. For instance, 2-butenoic acid showed the weakest binding energy of -3.2 kcal/mol, with hydrogen bond interactions involving THR218, ALA220, ASP440, THR437, and ARG438, along with a hydrophobic interaction with TRP489. However, it lacked significant electrostatic interactions, which likely contributed to its weaker binding affinity. Similarly, propanedioic acid had a binding energy of -3.6 kcal/mol, forming hydrogen bonds with ALA220 and ARG438. However, it also presented an unfavorable interaction with ASP440, which likely contributed to its weaker overall binding. Additionally, 9-octadecenal (Z)- showed a binding energy of -4.4 kcal/mol, with hydrogen bond interactions with SER435, MET436, and THR437, and hydrophobic interactions with PHE182, TRP185, and LEU219. However, it also exhibited an unfavorable interaction with ASP440, which may destabilize the complex and contribute to its lower binding affinity. Compounds with lower binding energies tend to show weaker interactions with their targets, and the presence of unfavorable interactions can further reduce binding strength. Furthermore, weak binding affinities may be influenced by the geometry of the ligand-binding pocket; a poor fit could lead to weaker interactions and reduced overall binding strength. These compounds may require optimization to improve their interactions with the binding pocket and enhance their biological efficacy. This suggests that further refinement is needed to improve their binding affinities and potential therapeutic effectiveness.

The protein 6I1E, identified as penicillin-binding protein 3 (PBP3) in *P. aeruginosa*, plays a crucial role in bacterial cell wall synthesis, particularly in the transpeptidation step of peptidoglycan formation, which is essential for maintaining cell wall integrity. As such, PBP3 is a key target for antimicrobial therapies (Bellini et al. 2019). In in-vitro studies, *P. xanthinum* extract exhibited an inhibition zone of 11.53±0.11 mm against *P. aeruginosa*, supporting its antimicrobial potential, which is consistent with in-silico findings. Molecular docking studies with 6I1E showed that bioactive compounds from *P. xanthinum*, particularly benzenepropanoic acid, α-(2,5-dioxopyrrolo)-, demonstrated a binding energy of -5.9 kcal/mol, suggesting comparable inhibitory potential to the control compound. The strong binding affinity of these compounds is attributed to their ability to form hydrogen bonds and hydrophobic interactions with the active site of PBP3, effectively blocking the critical transpeptidation reaction. These results highlight promising leads for developing novel therapies to combat antibiotic-resistant bacteria.

This study underscores *P. xanthinum* as a key contributor to lichen biodiversity, with notable potential for antimicrobial applications due to its bioactive secondary metabolites. We investigated the biodiversity of *P. xanthinum*, focusing on its antimicrobial potential through both in vitro and in silico approaches. Methanol extracts of *P. xanthinum* were evaluated against Gram-positive and Gram-negative bacteria, as well as pathogenic yeast, using the disc diffusion method. The extracts exhibited significant antimicrobial activity, particularly against *E. coli* (18.6±0.44 mm) and *S. enterica* serovar Typhi (15.8±0.25 mm). Gas chromatography-mass spectrometry (GC-MS) analysis identified 29 bioactive compounds, and their drug-likeness was assessed according to Lipinski's rule of five. Molecular docking studies with penicillin-binding protein 3 from *P. aeruginosa* (6I1E) revealed strong binding affinities for compounds such as benzenepropanoic acid, α-(2,5-dioxopyrrolo)- (-5.9 kcal/mol) and 2,2,3,3-tetramethylcyclopropanoic acid, phenyl ester (-5.2 kcal/mol), highlighting their promising potential as antimicrobial agents. These findings reinforce the value of *P. xanthinum* as a rich source of bioactive compounds, which can be further explored for the development of novel antimicrobial therapies. This study contributes to the growing body of knowledge on lichen-derived metabolites and their mechanisms of action, providing a strong foundation for future research aimed at optimizing these compounds for clinical use. The added value of this research lies in its comprehensive approach, integrating in vitro, in silico, and analytical techniques, offering a robust framework for exploring the antimicrobial potential of lichen species. This work makes a significant contribution to the expanding field of bioactive compound research, presenting new opportunities to address antimicrobial resistance and promote the use of natural resources in drug development.

ACKNOWLEDGEMENTS

This work was supported by the Ministry of Education, Culture, Research and Technology, Republic of Indonesia, under a PMDSU Research Grant (Contract Number: 88/UN5.4.10. S/PPM/KPDRTPM/2024).

REFERENCES

Alzayn M, Dulyayangkul P, Satapoomin N, Heesom KJ, Avison MB. 2021. Ompf downregulation mediated by sigma E or OmpR activation confers cefalexin resistance in *Escherichia coli* in the absence of acquired β-lactamases. Antimicrob Agents Chemother 65 (11): 1110-1128. DOI: 10.1128/aac.01004-21.

Atni OK, Munir E, Siregar ES, Saleh M. 2024. Lichen diversity and taxonomy in Bukit Barisan Grand Forest Park, North Sumatra, Indonesia. Biodiversitas 25: 1623-1630. DOI: 10.13057/biodiv/d250431.

Badiali C, Petruccelli V, Brasili E, Pasqua G. 2023. Xanthones: Biosynthesis and trafficking in plants, fungi and lichens. Plants 12 (4): 694. DOI: 10.3390/plants12040694.

Bellini D, Koekemoer L, Newman H, Dowson CG. 2019. Novel and improved crystal structures of *H. influenzae*, *E. coli* and *P. aeruginosa* penicillin-binding protein 3 (PBP3) and *N. gonorrhoeae* PBP2: Toward a better understanding of β-lactam target-mediated resistance. J Mol Biol 431 (18): 3501-3519. DOI: 10.1016/j.jmb.2019.07.010.

Chakarwarti J, Anand V, Nayaka S, Srivastava S. 2024. In vitro antibacterial activity and secondary metabolite profiling of endolichenic fungi isolated from genus *Parmotrema*. Curr Microbiol 81 (7): 195. DOI: 10.1007/s00284-024-03719-4.

Chen W, Zhang YM, Davies C. 2017. Penicillin-binding protein 3 is essential for growth of *Pseudomonas aeruginosa*. Antimicrob Agents Chemother 61 (1): 10-1128. DOI: 10.1128/aac.01651-16.

Choi U, Lee CR. 2019. Distinct roles of outer membrane porins in antibiotic resistance and membrane integrity in *Escherichia coli*. Front Microbiol 10: 953. DOI: 10.3389/fmicb.2019.00953.

Cunrath O, Meinel DM, Maturana P, Fanous J, Buyck JM, Saint Auguste P, Seth-Smith HMB, Körner J, Dehio C, Trebosc V, Kemmer C, Neher R, Egli A, Bumann D. 2019. Quantitative contribution of efflux to multi-drug resistance of clinical *Escherichia coli* and *Pseudomonas aeruginosa* strains. EBioMedicine 41: 479-487. DOI: 10.1016/j.ebiom.2019.02.061 2352-3964.

Dandapat M, Paul S. 2019. Secondary metabolites from lichen *Usnea longissima* and its pharmacological relevance. Pharmacogn Res 11 (2): 103-109. DOI: 10.4103/pr.pr_111_18.

Dwarakanath PR, Abinaya K, Nagasathya K, Meenakumari S, Gopinath SC, Raman P. 2022. Profiling secondary metabolites from lichen "*Parmotrema perlatum* (Huds.) M. Choisy" and antibacterial and antioxidant potentials. Biomass Convers Biorefin 14 (14): 16461-16471. DOI: 10.1007/s13399-022-03572-0.

Farrag HA, Abdallah N, Shehata MM, Awad EM. 2019. Natural outer membrane permeabilizers boost antibiotic action against irradiated resistant bacteria. J Biomed Sci 26: 96. DOI: 10.1186/s12929-019-0561-6.

Galindo-Méndez M. 2020. *E. coli* Infections-Importance of Early Diagnosis and Efficient Treatment. IntechOpen, London. DOI: 10.5772/intechopen.80139.

Goga M, Elečko J, Marcinčinová M, Ručová D, Bačkorová M, Bačkor M. 2020. Lichen metabolites: An overview of some secondary metabolites and their biological potential. In: Mérillon JM, Ramawat K (eds). Co-evolution of secondary metabolites. Springer, New York. DOI: 10.1007/978-3-319-96397-6_57.

Gómez-Serranillos MP, Fernández-Moriano C, González-Burgos E, Divakar PK, Crespo A. 2014. Parmeliaceae family: Phytochemistry, pharmacological potential and phylogenetic features. Rsc Adv 4 (103): 59017-59047. DOI: 10.1039/c4ra09104c.

Ivanović V, Rančić M, Arsić B, Pavlović A. 2020. Lipinski's rule of five, famous extensions and famous exceptions. Pop Sci Article 3 (1): 171-177. DOI: 10.46793/chemn3.1.171i.

Karami TK, Hailu S, Feng S, Graham R, Gukasyan HJ. 2022. Eyes on Lipinski's rule of five: A new "rule of thumb" for physicochemical design space of ophthalmic drugs. J Ocular Pharmacol Therapeut 38 (1): 43-55. DOI: 10.1089/jop.2021.0069.

Kello M, Goga M, Kotorova K, Sebova D, Frenak R, Tkacikova L, Mojzis J. 2023. Screening evaluation of antiproliferative, antimicrobial and antioxidant activity of lichen extracts and secondary metabolites in vitro. Plants 12 (3): 611. DOI: 10.3390/plants12030611.

Lipinski CA, Lombardo F, Dominy BW, Feeney PJ. 1997. Experimental and computational approaches to estimate solubility and permeability in drug discovery and development settings. Adv Drug Deliv Rev 23 (1-3): 3-25. DOI: 10.1016/S0169-409X(96)00423-1.

Lücking R, Hodkinson BP, Leavitt SD. 2017. The 2016 classification of lichenized fungi in the Ascomycota and Basidiomycota-Approaching one thousand genera. J Bryol 119 (4): 361-416. DOI: 10.1639/0007-2745-119.4.361.

Macedo DCS, Almeida FJF, Wanderley MSO, Ferraz MS, Santos NPS, López AMQ, Lira-Nogueira MCB, 2021. Usnic acid: From an ancient lichen derivative to promising biological and nanotechnology applications. Phytochem Rev 20: 609-630. DOI: 10.1007/s11101-020-09717-1.

Maulidiyah M, Darmawan A, Usman U, Musdalifah A, Ode L, Salim A, Nurdin M, 2021. Antioxidant activity of secondary metabolite compounds from lichen *Teloschistes flavicans*. Biointerface Res Appl Chem 11: 13878-13884. DOI: 10.1088/1742-6596/1763/1/012068.

Mendili M, Khadhri A, Mediouni-Ben Jemâa J, Andolfi A, Tufano I, Aschi-Smiti S, DellaGreca M, 2022. Anti-inflammatory potential of compounds isolated from Tunisian lichens species. Chem Biodiver 19 (8): e202200134. DOI: 10.1002/cbdv.202200134.

Millot M, Dieu A, Tomasi S, 2016. Dibenzofurans and derivatives from lichens and ascomycetes. Nat Prod Rep 33 (6): 801-811. DOI: 10.1039/c5np00134j.

Nguyen TTS, Yoon Y, Yang HB, Lee S, Oh MH, Jeong JJ, Kim ST, Yee F, Crisan C, Moon KY, Lee KK, Kim JS, Hur, H Kim. 2014. Lichen secondary metabolites in *Flavocetraria cucullata* exhibit anti-cancer effects on human cancer cells through the induction of apoptosis and suppression of tumorigenic potentials. PLoS One 9 (10): e111575. DOI: 10.1371/journal.pone.0111575.

Ozturk S, Erkisa M, Oran S, Ulukaya E, Celikler S, Ari F, 2021. Lichens exerts an antiproliferative effect on human breast and lung cancer cells through induction of apoptosis. Drug Chem Toxicol 44 (3): 259-267. DOI: 10.1080/01480545.2019.1573825.

Prajapati JD, Kleinekathöfer U, Winterhalter M. 2021. How to enter a bacterium: Bacterial porins and the permeation of antibiotics. Chem Rev 121 (9): 5158-5192. DOI: 10.1021/acs.chemrev.0c01213.

Ranković B, Kosanić M. 2019. Lichens as a potential source of bioactive secondary metabolites. In: Ranković B (eds). Lichen secondary metabolites: Bioactive properties and pharmaceutical potential. Springer, New York. DOI: 10.1007/978-3-030-16814-8_1.

Ranković B, Kosanić M. 2021. Biotechnological substances in lichens. In: Sinha RP, Häder D-P (eds). Natural Bioactive Compounds Technological Advancements. Academic Press, Cambridge. DOI: 10.1016/B978-0-12-820655-3.00012-4.

Saha S, Pal A, Paul S. 2021. A review on pharmacological, antioxidant activities and phytochemical constituents of a novel lichen *Parmotrema* species. J Biol Active Prod Nat 11 (3): 190-203. DOI: 10.1080/22311866.2021.1916596.

Shiromi PSAI, Hewawasam RP, Jayalal RGU, Rathnayake H, Wijayaratne WMDGB, Wanniarachchi D. 2021. Chemical composition and antimicrobial activity of two Sri Lankan lichens, *Parmotrema rampoddense*, and *Parmotrema tinctorum* against methicillin-sensitive and methicillin-resistant *Staphylococcus aureus*. Evid Based Complement Alternat Med 2021: 9985325. DOI: 10.1155/2021/9985325.

Smith JL, Fratamico PM, Gunther IV NW. 2014. Shiga toxin-producing *Escherichia coli*. Adv Appl Microbiol 86: 145-197. DOI: 10.1016/B978-0-12-800262-9.00003-2.

Tatipamula VB, Tatipamula VK, 2021. Dibenzofurans from *Cladonia corniculata* Ahti and Kashiw inhibit key enzymes involved in inflammation and gout: An in vitro approach. Indian J Chem Sect B 60: 715-719. DOI: 10.56042/ijcb. v60i5. 38966.

Thakur R, Suri CR, Rishi P. 2022. Contribution of typhoid toxin in the pathogenesis of *Salmonella Typhi*. Microb Pathog 164: 105444. DOI: 10.1016/j.micpath.2022.105444.

Tuan NT, Dam NP, Van Hieu M, Trang DTX, Danh LT, Men TT, De TQ, Bach LT, Kanaori K. 2020. Chemical constituents of the lichen *Parmotrema tinctorum* and their antifungal activity. Chem Nat Compd 56: 315-317. DOI: 10.1007/s10600-020-03017-y.

Ureña-Vacas I, Burgos EG, Divakar PK, Gómez-Serranillos MP. 2021. Dibenzofurans from lichens-a pharmacological overview. Curr Top Med Chem 21: 2397-2408. DOI: 10.2174/1568026621666210728095214.

Weerakoon G, Aptroot A. 2014. Over 200 new lichen records from Sri Lanka, with three new species to science. Cryptogamie Mycologie 35 (1): 51-62. DOI: 10.7872/crym.v35.iss1.2014.51.

Zermeño-Cervantes LA, Martínez-Díaz SF, Venancio-Landeros AA, Cardona-Félix CS. 2023. Evaluating the efficacy of endolysins and membrane permeabilizers against *Vibrio parahaemolyticus* in marine conditions. Res Microbiol 174 (7): 104104. DOI: 10.1016/j.resmic.2023.104104.